

Article ID: 1006-8775(2013) 04-0331-09

## SIMULATING THE RESPONSE OF NON-UNIFORMITY OF PRECIPITATION EXTREMES OVER CHINA TO CO<sub>2</sub> INCREASING BY MIROC\_HIRES MODEL

ZHU Jian (朱 坚)<sup>1,2</sup>, HUANG Dan-qing (黄丹青)<sup>3</sup>, ZHOU Peng (周 鹏)<sup>3,4</sup>, LIN Hui-juan (林惠娟)<sup>5</sup>

(1. State Key Laboratory of Hydrology-Water Resources and Hydraulics Engineering, College of Hydrology and Water Resources, Hohai University, Nanjing 210098 China; 2. Key Laboratory of Meteorological Disaster of Ministry of Education, Nanjing University of Information Science and Technology, Nanjing 210044 China; 3. School of Atmospheric Sciences, Nanjing University, Nanjing 210093 China; 4. State Key Laboratory of Loess and Quaternary Geology, Institute of Earth Environment, Chinese Academy of Sciences, Xi'an 710075 China; 5. Nanjing Meteorological Bureau, Suzhou 215021 China)

**Abstract:** The response of non-uniformity of precipitation extremes over China to doubled CO<sub>2</sub> has been analyzed using the daily precipitation simulated by a coupled general circulation model, MIROC\_Hires. The major conclusions are as follows: under the CO<sub>2</sub> increasing scenario (SRES A1B), the climatological precipitation extremes are concentrated over the southern China, while they are uniformly distributed over the northern China. For interannual variability, the concentration of precipitation extremes is small over the southern China, but it is opposite over the northern China. The warming effects on the horizontal and vertical scales are different over the northern and southern part of China. Furthermore, the atmospheric stability is also different between the two parts of China. The heterogeneous warming is one of the possible reasons for the changes in non-uniformity of precipitation extremes over China.

**Key words:** precipitation extremes; concentration density and period; CO<sub>2</sub> increase; asymmetric pattern

**CLC number:** P626.62

**Document code:** A

### 1 INTRODUCTION

Increased emission of greenhouse gas due to human activities has resulted in significant changes in temperature and precipitation, affecting the global climate. Because the impacts of climate change are evidently manifested in variations of intensity and frequency in the extremes, climate extremes attract more and more attention from scientists<sup>[1-6]</sup>. It is well known that climate models are powerful tools to investigate the past, present, and future climate change<sup>[7-10]</sup>. The possible change in the precipitation extremes (PEs) was simulated by various climate models under the scenarios of increased greenhouse gas. Meehl et al.<sup>[11]</sup> found that the spatial distribution of PEs intensity increment is apparently not symmetric. Turne et al.<sup>[12]</sup> indicated that in the 2×CO<sub>2</sub>

scenario, the averaged rainfall in summer increases slightly, especially over the central and northern India. In addition, the frequency of PEs is approximately doubled over the northern India to increase the occurrence probability of damaging floods. Marengo et al.<sup>[13]</sup> demonstrated that a significant increasing trend exists in both the intensity of PEs and the total rainfall. The evolution of PEs under 2×CO<sub>2</sub> forcing was investigated by Feng et al.<sup>[14]</sup> using a high-resolution GCM (Global Climate Model). The results pointed out that PE has different evolution in different regions. The frequency increases over the whole China with the increased intensity in most of the southeastern coastal area. Significant differences of PEs intensity in summer exist among regions in China. Li et al.<sup>[15]</sup> analyzed the variation of PE based

**Received** 2012-12-14; **Revised** 2013-09-18; **Accepted** 2013-10-15

**Foundation item:** National Basic Research Program of China (973 Program, 2012CB955901); National Natural Science Foundation of China (51190090); Open Project Program of State Key Laboratory of Loess and Quaternary Geology, Institute of Earth Environment (SKLLQG1308); National Natural Science Foundation of China (41105044, 41205038); Key Laboratory of Meteorological Disaster of Ministry of Education, Nanjing University of Information Science and Technology (KLME1201); Fundamental Research Funds for the Central Universities (2012B00114)

**Biography:** ZHU Jian, lecturer, primarily undertaking research on regional climate change and simulation.

**Corresponding author:** HUANG Dan-qing, e-mail: huangdq@nju.edu.cn

on the Coupled GCMs (CGCMs) with increased CO<sub>2</sub> forcing. The results presented larger regional differences in June and July. Jiang et al.<sup>[16]</sup> compared the predicted precipitation extreme events and found that PEs in China would be more frequent in the 21st century. In addition, the intensity of PEs and the extent of drought will increase, implying heavier rainfall and more rainfall-free days, and their trends are proportional to the intensity of greenhouse gas emission. Overall, the results mentioned above revealed that the PEs vary in different regions under the warming scenario. Both the frequency of PEs and drought days increase over all regions, indicating that the disastrous climate tends to be more severe.

It has already been an important climate change issue that whether the changes in PEs are due to global warming. The increasing of CO<sub>2</sub> density will firstly change the climate background. Then under the varied background, the PEs will change. However, is the raising rate of temperature the same in different regions under the increasing of CO<sub>2</sub>? Will the different increasing rate lead to non-uniform climate background? Will the changed background affect the evolution of PEs? These issues are still unsolved and worthy working on.

Analyses on extreme events are mostly concentrated on the parameters of frequency and intensity. If both the frequency and intensity are very large in one period, the concentrated rainfall will be very likely to cause floods. As in the Yangtze River (YR) region, the precipitation is featured by asymmetric temporal and spatial distributions. Floods in YR region are mainly caused by PEs, especially in July and August. If the PEs occur over the whole region simultaneously, the upstream flows may meet up with downstream flows and result in severe floods, such as the cases of 1954 and 1998. Otherwise, the rising flows come at different time and there may be no floods. Therefore, it is important to examine the non-uniformity of the PEs. Although many studies have been conducted on the PEs, few pays attention to the non-uniformity of PEs. Especially as the greenhouse gas emission increases, are the PEs more concentrated or more scattered and is it related to the global warming? Those are still issues to be solved. Then based on the outputs by MIROC\_Hires (a coupled general circulation model) provided by Intergovernmental Panel for Climate Change (IPCC) AR4<sup>[17]</sup>, the response of non-uniformity of PEs to the increased CO<sub>2</sub> and the possible mechanism are investigated in this study.

## 2 DATA AND METHODS

### 2.1 Model introduction

MIROC\_Hires model is a high resolution ocean-atmosphere coupled climate model developed

jointly by three Japanese institutions: the Center for Climate System Research (CCSR) of the University of Tokyo, the National Institute for Environmental Studies (NIES), and the Frontier Research Center for Global Change, Japan Agency for Marine-Earth Science and Technology (FRCGC). The model has a horizontal resolution of T106 spectral truncation (~100 km transform grid) and 56 vertical levels with relatively finer vertical resolution in the planetary boundary layer and around the tropopause for the atmosphere, 1/4° × 1/6° and 48 levels for the ocean and sea ice, and a 0.5° × 0.5° grid and 5 soil layers for the land. The model can well simulate precipitation over East Asia<sup>[18-21]</sup>. The model integrates from a pre-industrial state to a stable status and then continues running from 1900 to 2100. Continued historical climate forcing ends at 2000, and since 2001 the model has been running under SRES A1B scenario of greenhouse gas emission provided by IPCC. The daily precipitation of MIROC\_Hires outputs from 1961 to 2000 (hereafter referred to as “20C3M runs”) and from 2081 to 2100 (hereafter referred to as “A1B runs”) are used in this work.

### 2.2 Definition of precipitation extremes

Only one threshold is usually used to define the PEs in a year. Thus the PEs occur mostly in summer, less frequently in spring and autumn, and rarely in winter. To know more about the seasonal variation of PEs, a monthly threshold is adopted to identify the PEs in each month<sup>[22]</sup>. In the 20C3M run, the daily precipitation of each month from 1961 to 2000 is sorted from weak to strong and the threshold is the 90th percentage value, which is the value within the top 10%. On each grid, the daily rainfall exceeding the threshold is defined as a PE event. PE frequency (PEF) is the times of PEs occurring in a period and the PE intensity (PEI) is defined as the ratio of precipitation intensity minus the threshold value to the frequency. Here we use the same threshold value in the A1B run for comparing the results between the two simulations.

### 2.3 Definition of non-uniformity

The non-uniformity of PEs is characterized by precipitation concentration degree (PCD) and precipitation concentration period (PCP). The basic principle for calculating the PCD and PCP is vector analysis which considers the vector of PEI in both horizontal and vertical direction. For detailed calculation, refer to Zhu et al.<sup>[23]</sup> and Huang et al.<sup>[24]</sup>. The PCD indicates whether the PEs are concentrated and the PCP is the time when the maximum precipitation takes place. They are independent concepts, which can better illustrate the uniform characteristics of PEs.

## 2.4 Definition of stability

Stability is defined as a decreasing ratio of temperature to altitude, as  $\gamma = \frac{dT}{dz}$ . When the ratio is larger, the atmosphere is more unstable. In this article, the atmospheric column between 700 hPa and 300 hPa is chosen to calculate the stability.

## 3 RESULTS

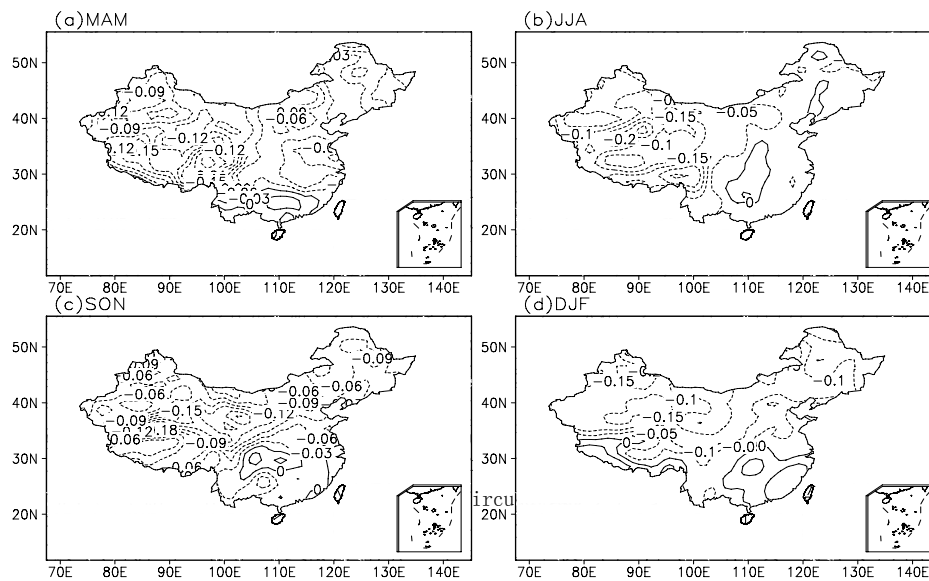


**Figure 1.** Difference of climatological CD of PEs over China between 20C3M and A1B runs. (a): MAM; (b): JJA; (c): SON; (d): DJF.

In spring (Fig. 2a), positive differences are over Xinjiang, Northeastern China and Southwestern China, implying the later occurrence of strong PEs in those regions under the increased CO<sub>2</sub> scenario. In summer (Fig. 2b), strong PEs appear later in Northeastern China, central Inner Mongolia Autonomous Region, and Southwestern China in the A1B run. In autumn (Fig. 2c), positive anomalies locate in most parts of China, especially in Xinjiang, North China and the Yangtze Delta. In winter (Fig. 2d), positive anomaly is located in Xinjiang and Southwestern China. It is found that strong PEs happen more obviously later with increased CO<sub>2</sub> in positive-anomaly regions in autumn and winter than in spring and summer, as shown in comparisons of the four seasons. Besides, strong PEs occur earlier in North China.

## 3.2 Standard deviation

Except for the climatological difference, the interannual variation should also be an important characteristic for the PE with increased CO<sub>2</sub>. Based on the standard deviation, the variation extent in different years can be investigated to show the precipitation's concentration or scattering extent of PEs in some years.

Figure 3 shows the distribution of standard deviation

## 3.1 Annual mean

Figure 1 shows the differences of PCD distribution between the 20C3M runs and the A1B runs in the four seasons. Negative differences cover most of China, especially the northern and southwestern part of China, indicating the PCD is decreased in the A1B runs. However, the PCD is increased in the southern part of China, especially in South China in winter. Overall, under the increased CO<sub>2</sub> scenario, PEs are not concentrated in most parts of China except for South China in winter.

difference of PCD in the four seasons between the 20C3M and A1B runs. Similar distribution can be seen in the four seasons, with positive anomalies over most part of China and negative anomalies in the southern part. The center of positive anomalies is located over Inner Mongolia, Tibetan, North China, Northeastern China and Southwestern China. It indicates that with increased CO<sub>2</sub>, the PCD of PEs varies from year to year, which represents that in some years the PE is more concentrated while in some other years the PE appears more scattered in those regions. However, in Southern China the interannual variability of PCD of PE is less in A1B runs than in 20C3M runs. Among the four seasons, the interannual variability of PCD is larger in spring and winter than in summer and autumn.

Similar to Fig. 3, Fig. 4 shows the distribution of standard deviation difference of PCP. Positive anomalies indicate that the time of strong PE occurrence is different, which means in some years a strong PE occur earlier while it occurs later in other years. Besides, negative anomalies means the occurrence date of strong PE is closer from year to year. In spring, most parts of China show positive anomalies, especially in Xinjiang, Inner Mongolia and Northeast China. In summer, positive anomalies are mainly located over Inner Mongolia and

Northeast China. In autumn, positive anomalies appear in Northeastern and Southern China, while negative anomalies are situated over the regions north of Yangtze River. In winter, positive anomalies are located over

Yellow River basin and southeastern part of Guangdong, while negative anomalies stay over the southwestern part of China.

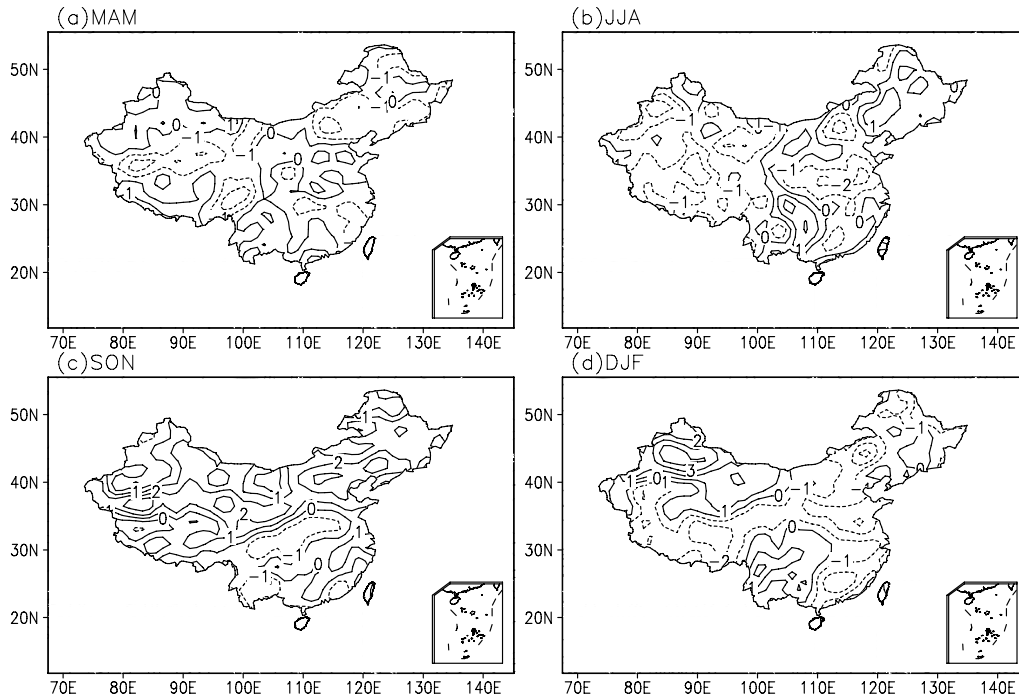


Figure 2. Same as Fig. 4, but for climatological CP of PEs.

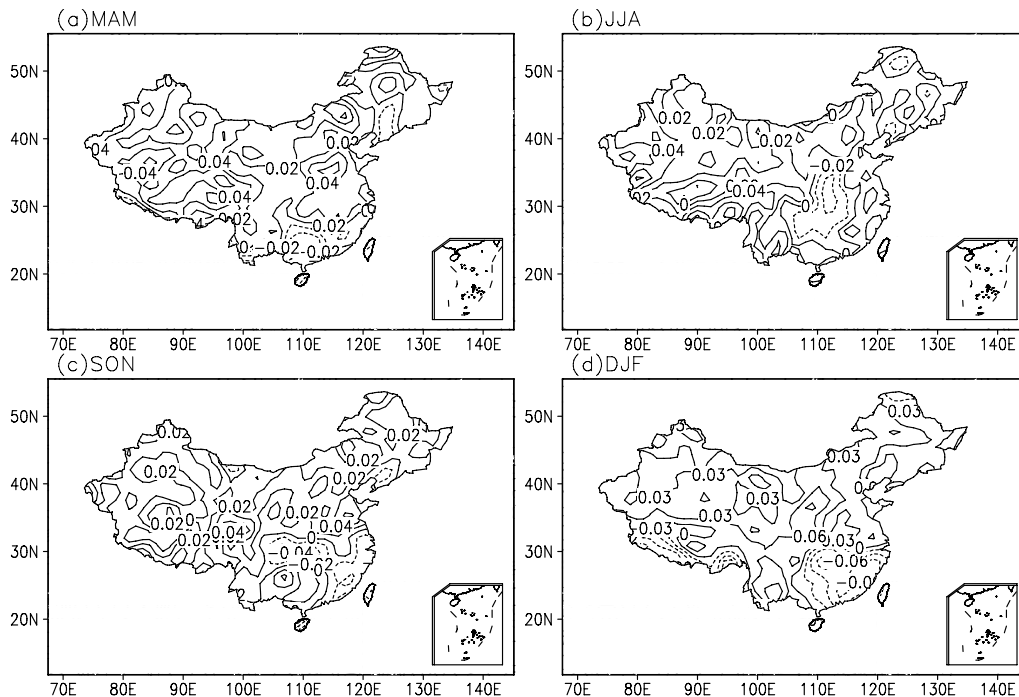


Figure 3. Same as Fig. 1 but for standard deviation CD of PEs.

### 3.3 Seasonal evolution over eastern China

Since precipitation is concentrated in East China, four sub-regions are examined to study their seasonal evolutions of the non-uniformity of PE. We divide East China into four parts<sup>[18]</sup>: Southern China (22-27°N,

110-120°E), Yantze-Huaihe River Basin (27-35°N, 110-122°E), Northern China (35-42°N, 110-120°E), and Northeastern China (42-52°N, 115-135°E).

Figure 5 depicts the seasonal evolution of PCD of PE averaged over the four regions. As shown in Fig. 5a, the large PCD is mainly in July and August in 20C3M

runs. While in A1B runs, the large values shift to January and February and become much larger. That means, over Southern China the PE is more scattered in warm seasons but more concentrated in cold seasons with increased CO<sub>2</sub>. However, over Yangtze-Huaihe region (Fig. 5b) the large values of PCD exist mainly in the period from previous October to February. PCD increases significantly in January and February in A1B

runs. In Fig. 5c and 5d, the large PCD values over Northern China and Northeastern China are in autumn and winter. In A1B runs, PCD decreases significantly, demonstrating the more scattered PE occurrence with increased CO<sub>2</sub>. Generally, in A1B runs the PCD decreases over northern China but increases over southern China.

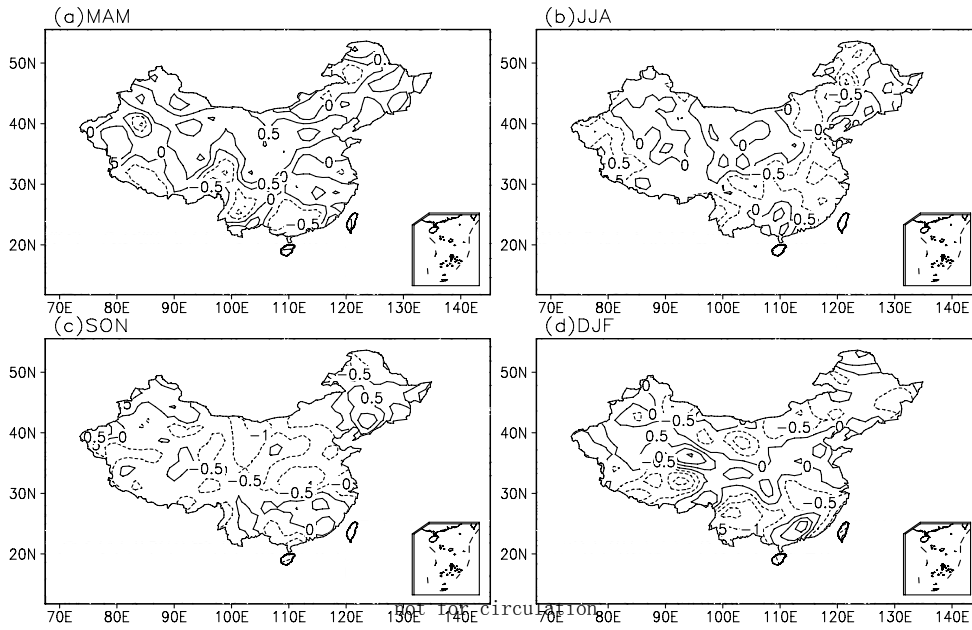


Figure 4. Same as Fig. 1 but for standard deviation CP of PEs.

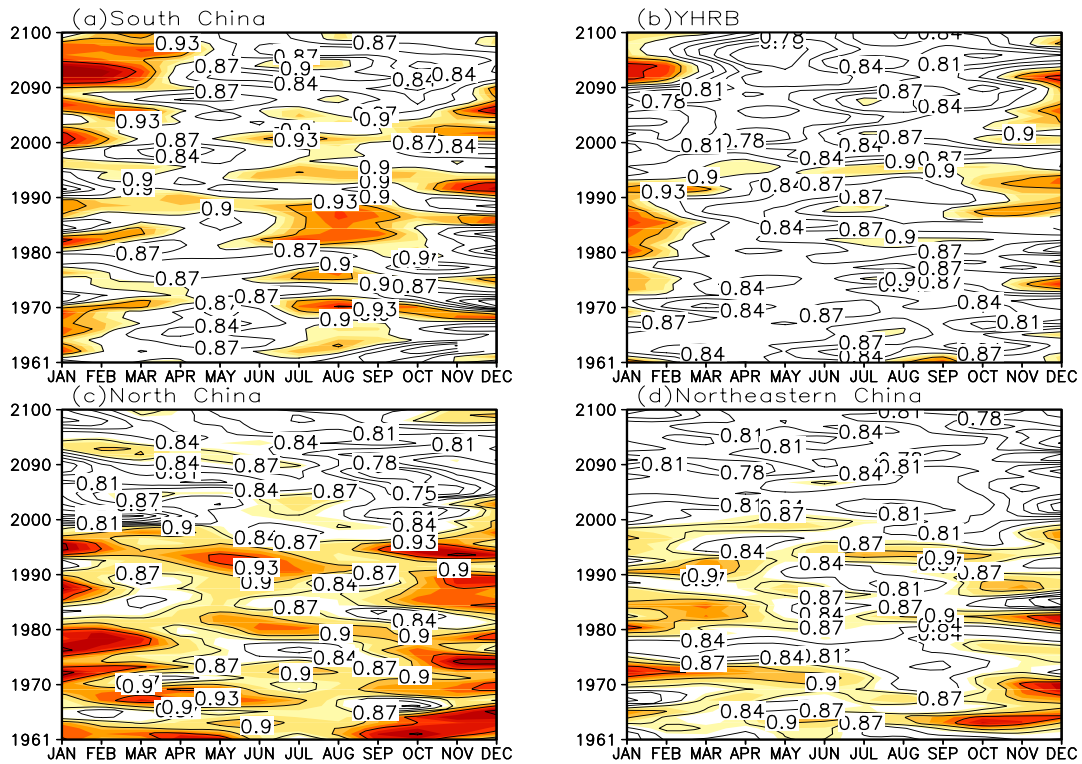


Figure 5. Seasonal evolution of regional CD of PEs over eastern China. (a): South China; (b): Yangtze-huaihe River; (c): North China; (d): Northeastern China. The shaded regions in (a), (b), (c), and (d) are values above 0.9, 0.9, 0.86, and 0.86, respectively.

Figure 6 is the same as Fig. 5 but for the PCP. In 20C3M runs, strong PE occurs late in spring (March to May) over Southern China before 1980 (Fig. 6a). After 1980, the occurrence of strong PE is late, mainly in January, February, and even in June to August. In A1B runs, the large centers primarily appear during May to August, which means strong PE occurs early in these months. As shown in Fig. 6b, the seasonal evolution of

PCP in the Yangtze-Huaihe region has almost the same feature as that over Southern China. In Fig. 6c, the strong PE happen late during October to December in both 20C3M and A1B runs. Over Northeastern China (Fig. 6d), large centers of PCP exist from March to May in 20C3M runs but from October to December in A1B runs.

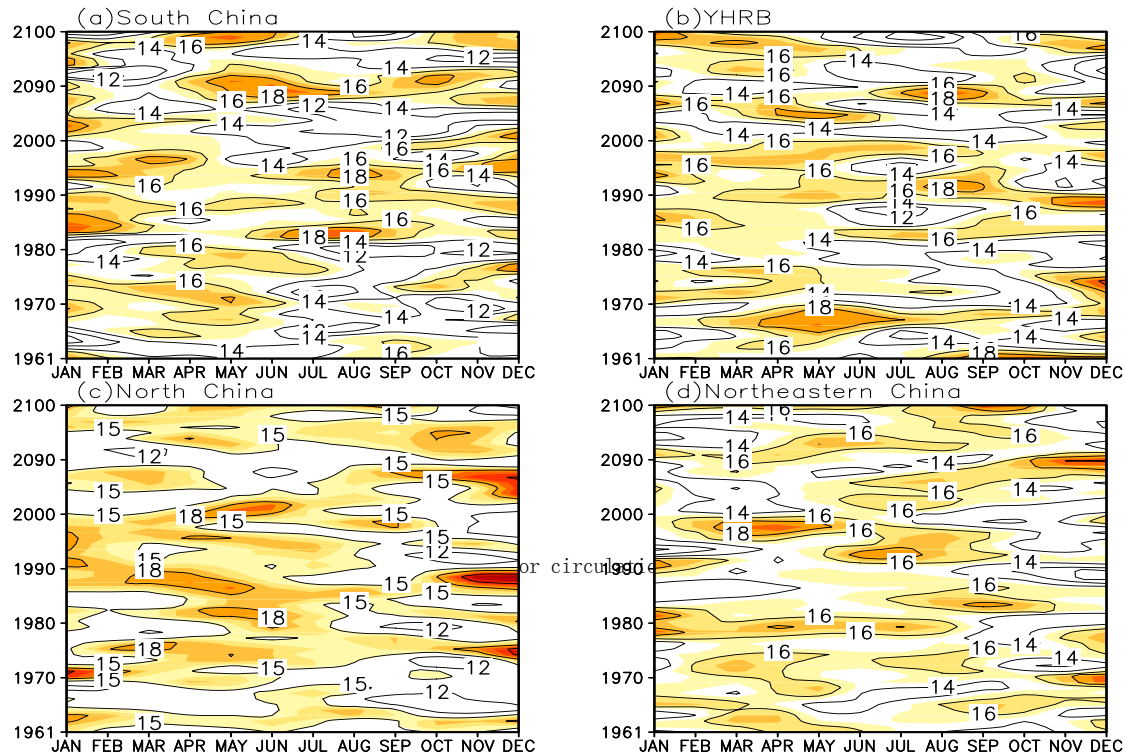


Figure 6. Same as Fig. 5 but for regional CP of PEs over eastern China.

#### 4 POSSIBLE ASSOCIATION BETWEEN NON-UNIFORM PE AND NON-UNIFORM WARMING

The analysis above indicates that large differences of non-uniform PE are located in southern and northern part of China with increased  $\text{CO}_2$ . In A1B runs, the PE over the southern part of China is more concentrated with small interannual variability. As is well known, the PE over the northern part of China is less concentrated but accompanied by large interannual variability with the increase of  $\text{CO}_2$ . As we know, with increased  $\text{CO}_2$ , the global temperature will increase in A1B runs. However, it is still unclear whether the warming in China is the same in different regions. Can the major reason for the non-uniformity of PE be the uneven warming between southern and northern part of China under the influence of global warming? Then the temperature difference (TD) in A1B and 20C3M runs on each layer is investigated to understand the temperature change with increased  $\text{CO}_2$ . The results show that the temperature on each layer rises with increased  $\text{CO}_2$  but the increasing magnitude is not similar for different regions and layers, which indicates

that uneven warming may exist in both horizontal and vertical directions. Since obvious north-south difference can be seen for PE, the meridional gradient of TD integrated from 1000 hPa to 200 hPa is given in Fig. 7. The distribution shows a “+ - +” pattern for TD from south to north in the four seasons. In detail, it is almost negative distribution of TD over regions at middle latitudes, especially in spring and autumn. As the meridional coordinate is oriented to the north, positive/negative TD means the warming magnitude is larger/smaller over the northern than over the southern regions. The distribution of “+ - +” TD indicates that the warming magnitude over the southern is not as large as over northern part of China. The different warming magnitude may be responsible for the non-uniformity of PEs.

Figure 8 shows the vertical distribution of TD between the two runs averaged for the four sub-regions. Significant differences can be seen between the southern and northern part of China. TD mostly increases with height over South China and Yangtze-Huaihe region. Especially in South China, TD all increases with longitude in the same trend for all the four seasons.

However, TD over North China and Northeast China increases more slowly with height than over the southern

part of China until 500 hPa and then it decreases quickly on the upper levels.

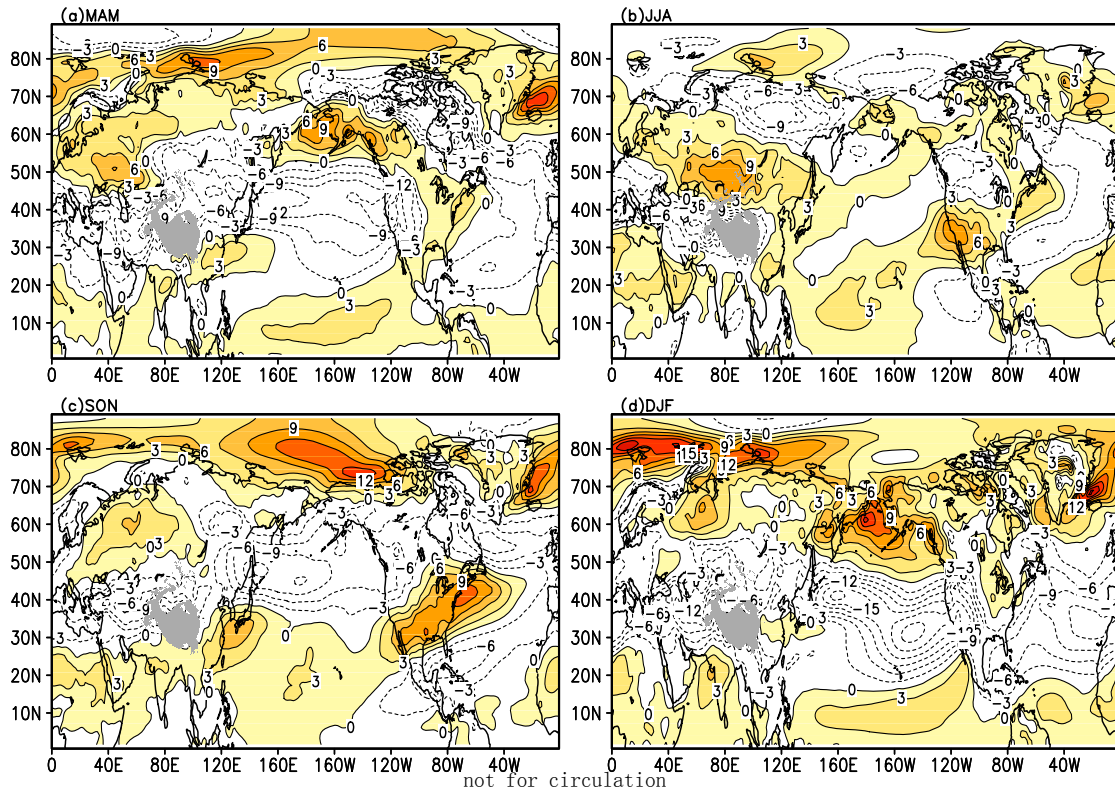


**Figure 7.** The difference of meridional temperature gradient between 20C3M and A1B runs integrated from 1000 to 200 hPa. (a): MAM; (b): JJA; (c): SON; (d): DJF. (Unit:  $\times 10^7$ ). Shaded regions are for the positive values.

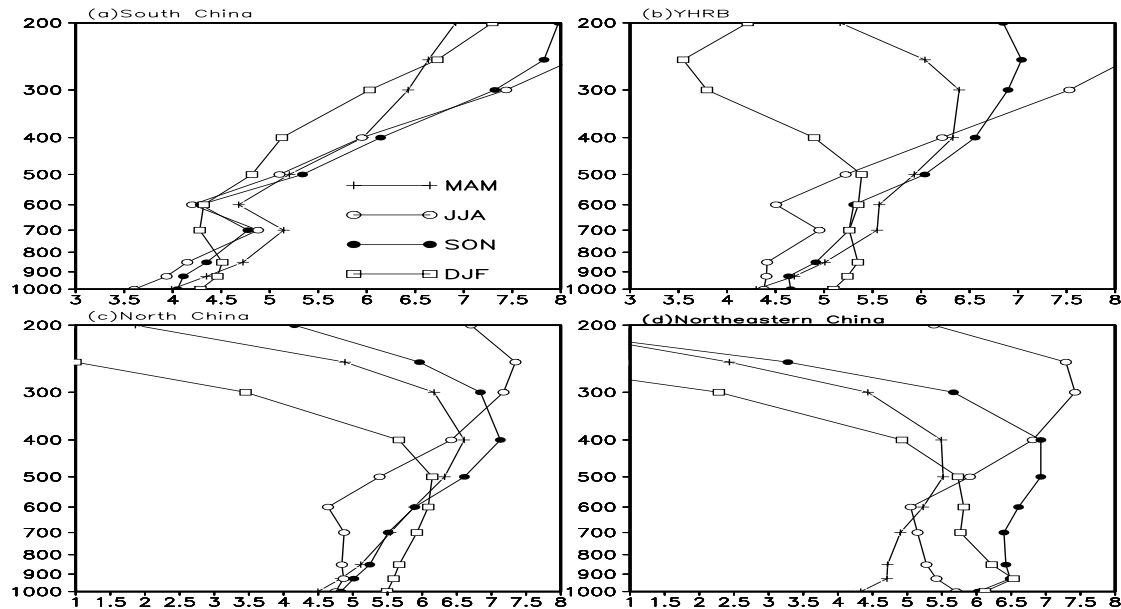


**Figure 8.** Difference of vertical structure of temperature between 20C3M and A1B runs in the four regions. (a): South China; (b): Yangtze-huaihe River; (c): North China; (d): Northeastern China. (Unit:  $^{\circ}\text{C}$ ).

Different warming magnitudes in the vertical direction may change the atmospheric stability. Thus the change in TD distribution can alter the stability distribution. Further comparison of the difference of static stability integrated from 700 to 300 hPa in the two

runs shows that strong meridional difference of stability significantly increases over the southern part of China in A1B runs (Fig. 9), indicating the more unstable atmosphere. Meanwhile, stability over the northern China is decreased so that the atmosphere stabilizes,

especially in spring, summer and winter. This is consistent with the distribution of more concentrated PEs in the southern part of China and more scattered PEs in the northern part, with increased  $\text{CO}_2$ .

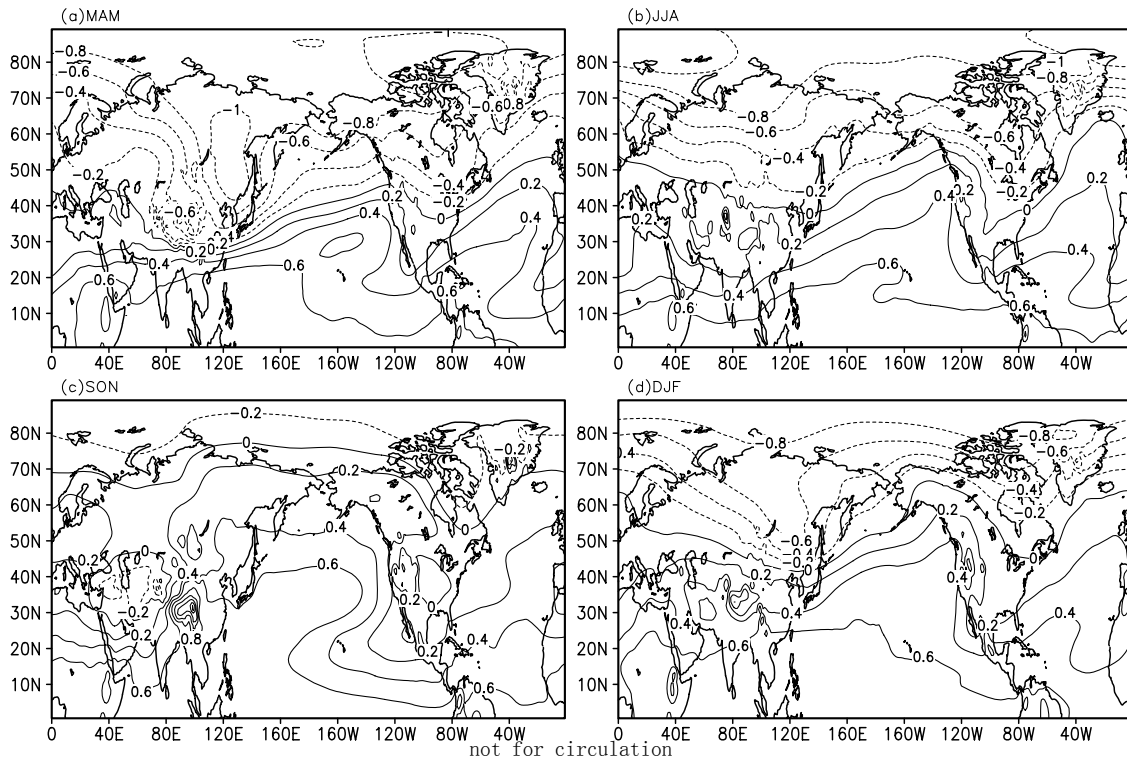


**Figure 9.** The difference of stability integrated from 700 to 300 hPa between 20C3M and A1B runs. (a): MAM; (b): JJA; (c): SON, (d): DJF. (Unit:  $\times 10^4$ ).

## 5 CONCLUSIONS

(1) For climatology, PEs are, with increased  $\text{CO}_2$ , more concentrated over the southern part of China, but more scattered over the northern part of China, especially over northwestern areas.

(2) The interannual variability of PCD is smaller in A1B runs than in 20C3M runs over the southern part of China, while it is larger in A1B runs over the northern part of China.

(3) For seasonal evolution, regional mean PCD over the northern part of China decreases with late occurrence of strong PEs. However, it increases in the southern part of China and strong PEs take place late during May to August.

(4) With increased  $\text{CO}_2$ , the horizontal and vertical warming extent is not the same. The warming extent in the horizontal is lower in the southern part of China than in the northern part. For the vertical distribution, the warming extent increases with height over the southern part of China, while it increases slowly with height until 500 hPa and then decreases quickly on the upper levels over the northern part of China. Because of the vertical asymmetric warming in different regions, the distribution of atmospheric instability anomaly shows a pattern of “+ - +” from south to north. Besides, this type is consistent with the non-uniformity of PEs over the southern and northern part of China.

This study is still a preliminary analysis based on the outputs of one coupled model. The conclusions are somewhat model dependent<sup>[25, 26]</sup>, and it is necessary to evaluate the response of other models participating in IPCC AR4 in simulation of the non-uniform pattern of PEs under the  $\text{CO}_2$  increasing scenario in the future.

## REFERENCES:

- [1] KIKTEV D, CAESAR J, ALEXANDER L V, et al. Comparison of observed and multi-modeled trends in annual extremes of temperature and precipitation [J]. *Geophys. Res. Lett.*, 2007, 34, L10702, doi:10.1029/2007GL029539.
- [2] MEEHL G A, ZWIERS F, EVANS J, et al. Trends in extreme weather and climate events: Issues related to modeling extremes in projections of future climate change [J]. *Bull. Amer. Meteor. Soc.*, 2000, 81(3): 427-436.
- [3] GROISMAN P, KARL T, EASTERLING D, et al. Changes in the probability of extreme precipitation: Important indicators of climate change [J]. *Clim. Change*, 1999, 42: 243-283.
- [4] WANG Xiao-ling, ZHAI Pan-mao. Changes in China's Precipitation in Various Categories during 1957~2004 [J]. *J. Trop. Meteor.*, 2008, 24(5): 459-466. (in Chinese)
- [5] LI Chun-hui, LIANG Jian-yin, WU Shang-sen. The characteristics of precipitation in the raining season in Guangzhou and its affecting factors over the past 100 years [J]. *J. Trop. Meteor.*, 2004, 20(4): 365-374. (in Chinese)
- [6] HUANG Dan-qing, QIAN Yong-fu, ZHU Jian. Trends of temperature extremes in China and their relationship with



- global temperature anomalies [J]. *Adv. Atmos. Sci.*, 2010 (27): 937-946.
- [7] EMORI S, HASEGAWA A, SUZUKI T, et al. Validation parameterization dependence and future projection of daily precipitation simulated with a high resolution atmospheric GCM [J]. *Geophys. Res. Lett.*, 2005: 32, L06708, doi : 10.1029/2004GL022306.
- [8] GROISMAN P Y, KARL T R, EASTERLING D R, et al. Changes in the probability of heavy precipitation: Important indicators of climatic change [J]. *Clim. Change*, 1999, 42: 243-283.
- [9] HARASAWA H. Comparison of the present day climate simulation over Asia in selected coupled atmosphere ocean global climate models [J]. *J. Meteor. Soc. Japan*, 2000, 78: 871-879.
- [10] YOU Feng-chun, ZHANG Hai-xia, ZHANG Yan-bin, et al. Forecast experiments of summer rainfall in China using Japanese general ocean-atmosphere coupled model [J]. *Plateau Meteor.*, 2007, 26 (5): 975 -979. (in Chinese)
- [11] MEEHL G, ARBLASTER J, TEBALDI C. Understanding future patterns of increased precipitation intensity in climate model simulations [J]. *Geophys. Res. Lett.*, 2005: 32, doi:10.1029/2005GL023680.
- [12] TURNER A G, SLINGO J M. Subseasonal extremes of precipitation and active-break cycles of the Indian summer monsoon in a climate-change scenario [J]. *Quart. J. Roy. Meteor. Soc.*, 2009, 135: 549-567.
- [13] MARENGO J A, JONES R, ALVES L M, et al. Future of change of temperature and precipitation extremes in South America as derived from the PRECIS regional climate modeling system [J]. *Int. J. Climatol.*, 2009, 29: 2241-2255.
- [14] FENG Lei, ZHOU Tian-jun, WU Bo, et al. Projection of future precipitation change over China with a high-resolution global atmospheric model [J]. *Adv. Atmos. Sci.*, 2010, 28: 464-476.
- [15] LI Hong-mei, FENG Lei, ZHOU Tian-jun, et al. Multi-model projection of July-August climate extreme changes over China under CO<sub>2</sub> doubling Part I: Precipitation [J]. *Adv. Atmos. Sci.*, 2010, 28: 433-447.
- [16] JIANG Zhi-hong, CHEN Wei-lin, SONG Jie, et al. Projection and evaluation of the precipitation extremes indices over China based on seven IPCC AR4 coupled climate models [J]. *Chin. J. Atmos. Sci.*, 2009, 33(1): 109-120. (in Chinese)
- [17] Intergovernmental Panel on Climate Change. IPCC AR4 Report [M]. Cambridge: Cambridge University Press, 2007.
- [18] ZHU Jian, ZHANG Yao-cun, HUANG Dan-qing. Analysis of Changes in Different-Class Precipitation over Eastern China under Global Warming [J]. *Plateau Meteor.*, 2009, 28(4): 889-896. (in Chinese).
- [19] ZHANG Y, TAKAHASHI M, GUO L L. Analysis of the East Asian subtropical westerly jet simulated by CCSR/NIES/FRCGC coupled climate system model [J]. *J. Meteor. Soc. Japan*, 2008, 86: 257-278.
- [20] K-1 Model Developers. K-1 coupled model (MIROC) description [R]. HASUMI H, EMORI S. Tokyo: University of Tokyo, 2004: 1, 34.
- [21] HUANG D, TAKAHASHI M, ZHANG Y C. Analysis of the Baiu precipitation and associated circulation simulated by the MIROC coupled climate system model [J]. *J. Meteor. Soc. Japan*, 2011, 89: 625-636.
- [22] MIN Shen, QIAN Yong-fu. Regionality of persistence of extreme precipitation events in China [J]. *Adv. Water Sci.*, 2008, 19(6): 763-771.
- [23] ZHU J, HUANG D Q, QIAN Y F, et al. Uneven characteristics of warm extremes during Meiyu period over Yangtze-Huaihe region and its configuration with circulation systems [J]. *Chin. J. Geophys.*, 2010, 53(10): 2310-2320. (in Chinese)
- [24] HUANG D Q, YONG F Q, JIAN Z. The heterogeneity of Meiyu rainfall over Yangtze-Huaihe River valley and its relationship with oceanic surface heating and intraseasonal variability [J]. *Theor. Appl. Climatol.*, 2012, 108: 601-611.
- [25] LI Bo, ZHOU Tian-jun. Projected climate change over China under SRES A1B scenario: Multi-model ensemble and uncertainties [J]. *Adv. Clim. Change Res.*, 2010, 6(4): 270-276. (in Chinese).
- [26] HUANG D Q, ZHU J, ZHANG Y C, et al. Uncertainties on the simulated summer precipitation over Eastern China from the CMIP5 models [J]. *J. Geophys. Res.*, DOI: 10.1002/jgrd.50695.

**Citation:** ZHU Jian, HUANG Dan-qing, ZHOU Peng et al. Simulating the response of non-uniformity of precipitation extremes over China to CO<sub>2</sub> increasing by MIROC\_HIRES model. *J. Trop. Meteor.*, 2013, 19(4): 331-339.